JVI Journals.ASM.org

Distribution and Dynamics of Transcription-Associated Proteins during Parvovirus Infection

Teemu O. Ihalainen,[a,b] Sami F. Willman,[a] Einari A. Niskanen,[a,c] Outi Paloheimo,[a] Hanna Smolander,[a,d] Juha P. Laurila,[a,e] Minna U. Kaikkonen,[f] and Maija Vihinen-Ranta[a]

Nanoscience Center, Department of Biological and Environmental Science, University of Jyväskylä, Finland[a]; Department of Health Sciences and Technology, Laboratory for Biologically Oriented Materials, ETH Zurich, Zurich, Switzerland[b]; Department of Biochemistry, Medical Genetics Cluster, Erasmus University Medical Center, Rotterdam, The Netherlands[c]; Department of Virology, Haartman Institute, University of Helsinki, Helsinki, Finland[d]; University of Turku, Turku, Finland[e]; and AI Virtanen Institute, Department of Biotechnology and Molecular Medicine, University of Eastern Finland, Kuopio, Finland[f]

Canine parvovirus (CPV) infection leads to reorganization of nuclear proteinaceous subcompartments. Our studies showed that virus infection causes a time-dependent increase in the amount of viral nonstructural protein NS1 mRNA. Fluorescence recovery after photobleaching showed that the recovery kinetics of nuclear transcription-associated proteins, TATA binding protein (TBP), transcription factor IIB (TFIIB), and poly(A) binding protein nuclear 1 (PABPN1) were different in infected and noninfected cells, pointing to virus-induced alterations in binding dynamics of these proteins.

In animals, several DNA viruses depend on host cell nuclear replication and transcription machinery (52). TATA binding protein (TBP) and transcription factor IIB (TFIIB) are key constituents of assembly of the host cell transcription initiation complex. Previous studies have shown that TBP interacts with viral transcription activators, including adenovirus EIA (21, 22, 32), hepatitis B virus pX and NS5A (38), herpes simplex virus 1 (HSV-1) VP16 (24, 34), human cytomegalovirus IE2 (23, 31, 49), and human immunodeficiency virus (HIV) Tat (30, 39, 48). The poly(A) binding protein nuclear 1 (PABPN1) accumulates to splicing speckles. It binds with high affinity to nascent poly(A) tails, thus stimulating their extension and controlling their length (27). Interaction of viral components with PABPN1 can lead to stimulated transcription (HSV-1 ICP27) (18, 19) or reduced host cell mRNA maturation and export (influenza A virus NS1) (9, 10). TAP and CRM1, essential export factors of nuclear mRNA, are also responsible for the nuclear export of HSV and influenza A virus mRNAs (8, 28, 40, 41). Moreover, promyelocytic leukemia (PML) nuclear bodies, involved in a wide variety of cellular processes, including regulation of transcription, interact with nuclear components of HSV-1 (35), polyomaviruses (29, 45), and parvoviruses (adeno-associated virus [AAV], minute virus of mice [MVM]) (20, 51).

Canine parvovirus (CPV) is a single-stranded DNA virus (46). Its nonstructural protein NS1 serves as an initiator and a helicase in viral DNA replication and as an activator of the viral promoters during diversion of the cellular machinery toward viral protein expression (11, 13, 36, 37).

We examined CPV infection-induced alterations in distribu-

Received 27 June 2012 Accepted 24 September 2012
Published ahead of print 3 October 2012
Address correspondence to Maija Vihinen-Ranta, maija.vihinen-ranta@jyu.fi.

doi:10.1128/JVI.01625-12

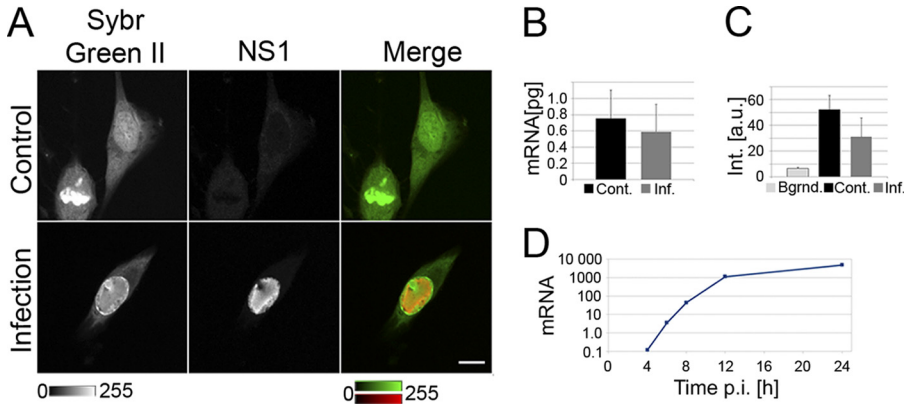

FIG 1 Detection of RNA synthesis in infected cells and RNA and mRNA quantification and NS1 RT-PCR analysis in noninfected and infected NLFK cells. (A) RNA distribution in noninfected and infected cells at 24 h p.i. Total RNA was labeled using SYBR green II (SG) and viral NS1 protein by indirect immunofluorescence. Bar, 10 μm. (B and C) mRNA isolation and quantification ($P > 0.05$) (B) and flow cytometric analysis of total RNA synthesis in noninfected (Cont.) and infected (Inf.) cells ($P < 0.01$) (C). RNA was labeled for flow cytometry using SYBR green II. Error bars indicate standard deviations. (D) Quantification of relative levels of NS1 mRNA synthesis by RT-PCR at 4 to 24 h p.i. As an endogenous control for the amount of template cDNA, 18S rRNA was used. Relative gene expression was measured as the ratio of the target to the 18S rRNA.

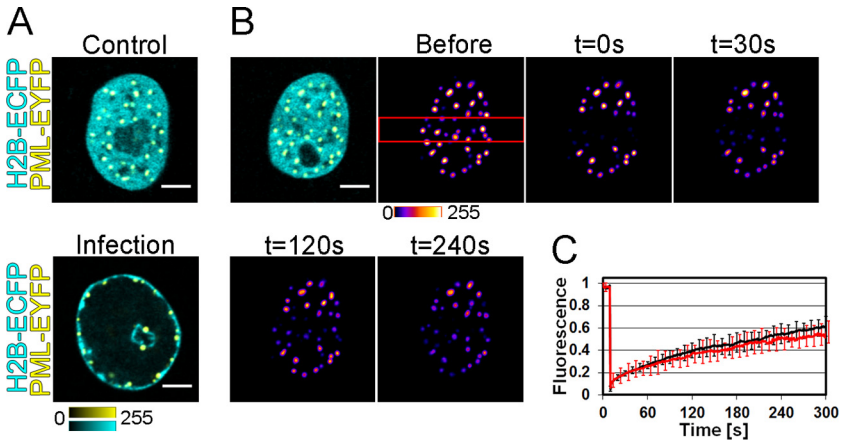

FIG 2 PML-EYFP binding and organization of PML bodies in nuclei. Qualitative FRAP experiments were performed in cells stably expressing H2B-EYFP and transiently expressing PML(IV)-EYFP. (A) Distributions of PML bodies [PML(IV)-EYFP, yellow] and chromatin (H2B-ECFP, cyan) in living noninfected and infected cells at 24 h p.i. (B) FRAP of PML(IV)-EYFP (yellow) in noninfected cells. Chromatin is visualized with H2B-ECFP (cyan). The red box denotes the bleach area of the FRAP experiment. Bars, 5 μm. (C) PML(IV)-EYFP fluorescence recovery in infected (red) and noninfected (black) cells. Error bars indicate standard deviations. The FRAP bleaching and imaging parameters were as follows: rectangular region bleaching of interest (ROI), 1.28 μm by 24.4 μm; bleaching iterations, 10; frame interval, 1,000 ms.

tion and dynamics of nuclear proteins associated with the transcription (TBP, TFIIB, PML), processing (PABPN1), and nuclear export (TAP) of mRNAs.

Synthesis of cellular mRNA and total RNA in infected cells was spectrophotometrically quantified by the use of purified mRNA and by image analysis of SYBR green II-labeled cytosolic RNA (Molecular Probes, Eugene, OR). The amount of cellular mRNA of infected cells at 24 h postinfection (p.i.) was similar to that of noninfected cells ($n = 16$, $P > 0.05$; Fig. 1B). Simultaneously, the amount of cytoplasmic total RNA was decreased in infected cells ($n = 9$, $P < 0.01$; Fig. 1C). In contrast, reverse transcription (RT)-PCR studies showed that the emergence of NS1 mRNA at 4 h p.i. was followed by its significantly increased synthesis at 12 h p.i. (Fig. 1D).

Our previous studies indicated that in CPV infection, part of the enhanced cyan fluorescent protein (ECFP)-PML foci were situated in close proximity to or colocalized with the CPV NS1 protein in infected cells. Here, we examined the virus-induced change

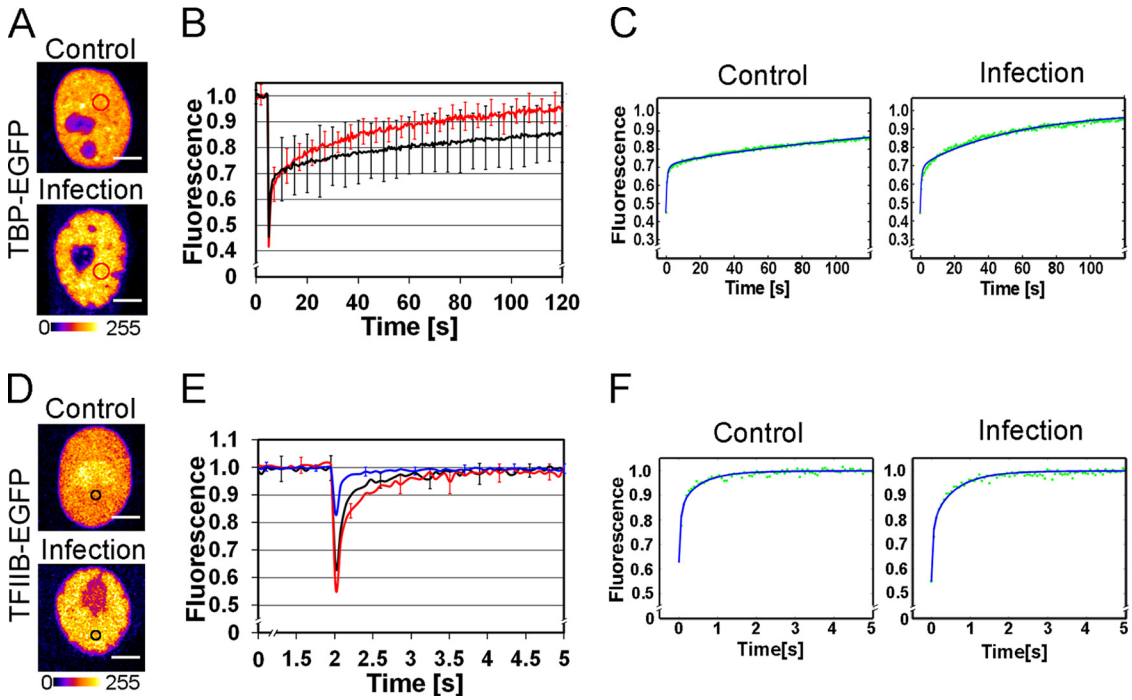

FIG 3 TBP-EGFP and TFIIB-EGFP dynamics are altered in virus infection. The results of confocal imaging and quantitative FRAP studies in cells stably expressing TBP-EGFP or TFIIB-EGFP fusion proteins are shown. (A and D) Live cell images of (A) TBP-EGFP and (D) TFIIB-EGFP distribution in the nuclei of noninfected and infected cells at 24 h p.i. Bars, 5 μm. (B) FRAP curves of TBP-EGFP in infected (red) and noninfected (black) cells. (E) FRAP curves of TFIIB-EGFP in infected (red) and noninfected (black) cells and EGFP in noninfected (blue) cells. (C, D, and F) TBP-EGFP and TFIIB-EGFP fluorescence recovery (green) data from noninfected and infected cells fitted into the FRAP model (blue). Errors bars indicate standard deviations. The FRAP bleaching and imaging parameters for TBP-EGFP/TFIIB-EGFP were as follows: circular ROIs with a radius of 1.34 ± 0.2 and 0.76 ± 0.15 μm; iterations, 10/8; frame intervals, 1,000/65 ms.

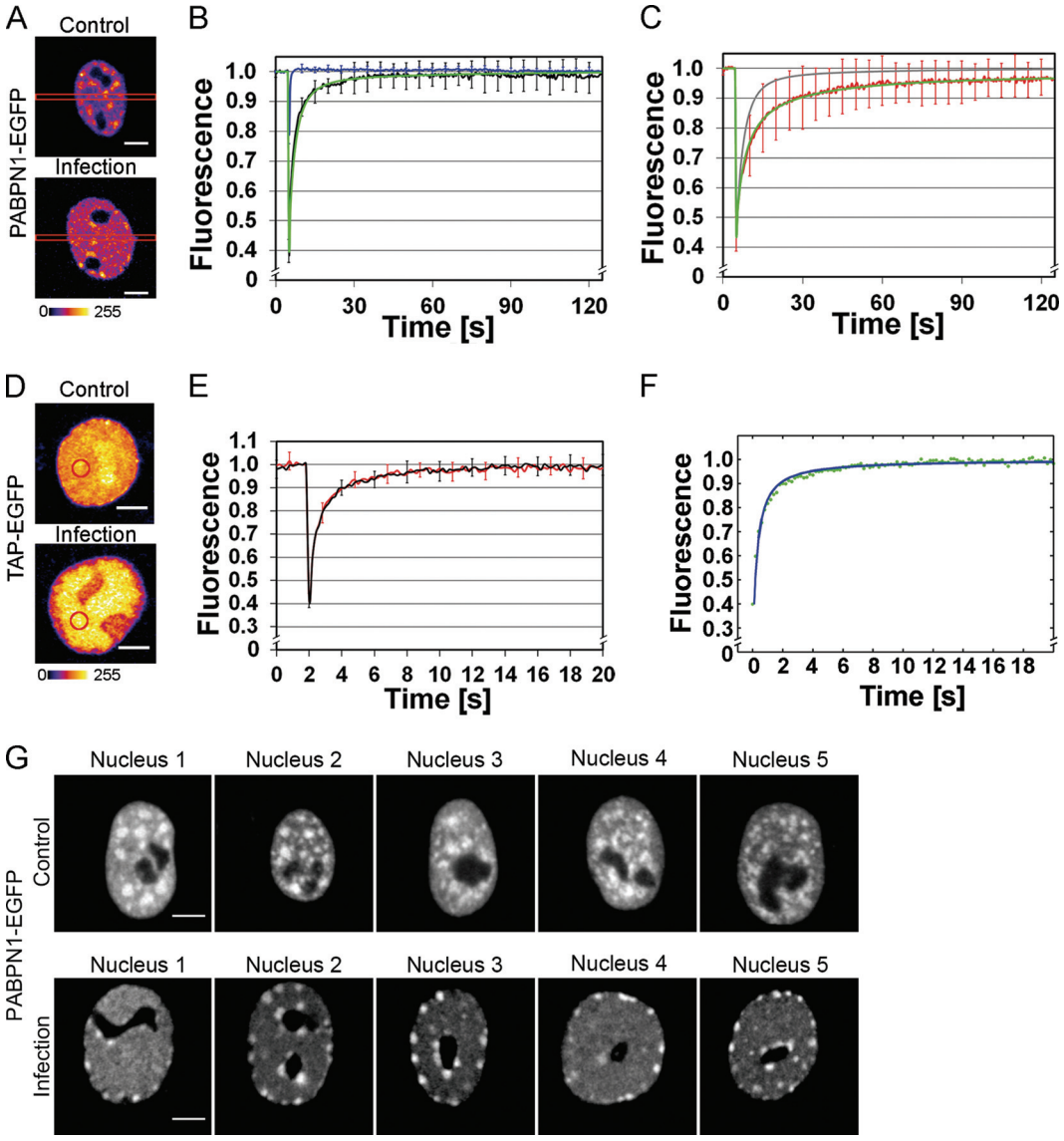

FIG 4 PABPN1-EGFP binding is increased and TAP-EGFP binding is unaltered in infection. Cells transiently expressing PABN1-EGFP or TAP-EGFP fusion proteins were examined using confocal imaging and FRAP analysis. (A and D) Confocal images of (A) PABN1-EGFP and (D) TAP-EGFP distribution in living noninfected and infected cells at 24 h p.i. Photobleached areas are denoted by red boxs and circles. (B) PABPN1-EGFP recoveries in noninfected cells. Levels of measured (black) and simulated (green) PABPN1-EGFP FRAP in noninfected cells are shown in comparison to those of free EGFP (blue). (C) PABPN1-EGFP recoveries in infected cells. Simulated slow diffusion of mRNA (blue) and higher mRNA binding on-rate (green) compared to PABPN1-EGFP recovery (red) in infected cells are shown. (E) Fluorescence recovery of TAP-EGFP in noninfected (black) and infected (red) cells. (F) The recovery (green) in the noninfected cell was fitted into the free diffusion model, yielding a good fit (blue). Error bars indicate standard deviations. FRAP bleaching and imaging parameters for PABPN1-EGFP/TAP-EGFP were as follows: circular ROIs with a radius of 0.7 ± 0.3 and 1.34 ± 0.2 μm; iterations, 8/10; frame intervals, 250/200 ms. (G) PABN1-EGFP distribution in various noninfected and infected cells at 24 h p.i. Bars, 5 μm.

in the distribution and dynamics of PML(IV)-EYFP (42). In the noninfected cells, the nuclear PML(IV)-EYFP foci were distributed evenly, whereas in infected cells, they were confined to the nuclear or nucleolar periphery (Fig. 2A). The times of fluorescence recovery after photobleaching (FRAP) in infected and noninfected cells were almost identical, suggesting that the PML(IV)-EYFP binding properties were not affected at late stages of infection (Fig. 2B and C). Detailed descriptions of the FRAP protocol employed in this study are provided by Ihalainen et al. (25).

The effect of infection on nuclear dynamics of TBP and TFIIB was studied by FRAP analysis. In the nuclei of noninfected cells, TBP-enhanced green fluorescent protein (EGFP) and TFIIB-EGFP (7) were distributed relatively homogeneously, with some nucleolar enrichment of TFIIB-EGFP. At 24 h p.i., both proteins accumulated in the replication body area (Fig. 3A, B, and D). The replication body area contains viral NS1 and cellular proliferating cell nuclear antigen (PCNA). This virus-induced nuclear structure covers the entire nucleus at 24 h p.i., with the exclusion of the nucleolus (14, 25, 26, 50). However, TBP-EGFP and TFIIB-EGFP showed different FRAP behavior characteristics. The recovery of TBP-EGFP was slower (Fig. 3B) than that of freely diffusing EGFP or TFIIB-EGFP (Fig. 3E). The diffusion coefficients of TBP-EGFP and TFIIB-EGFP were calculated using simple mass scaling of the EGFP diffusion coefficient. The TBP-EGFP free diffusion times in

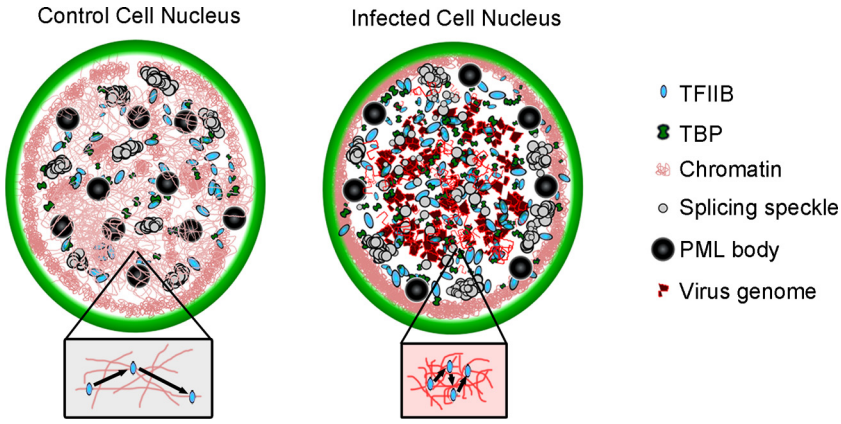

FIG 5 Schematic representation of infected cells. Images represent infected cells with an intranuclear distribution of nuclear and viral components at 24 h p.i in comparison with noninfected (control) cells.

noninfected and infected cells were 442 s and 147 s and the binding times 167 s and 58.8 s, respectively (Fig. 3C). The TFIIB-EGFP free diffusion times in noninfected and infected cells were 4.5 s and 3.0 s and the binding times 0.56 s and 0.63 s, respectively (Fig. 3F). These data indicate that TBP and TFIIB bind more frequently and are released faster in infected than noninfected cells.

Next, FRAP experiments were performed in PABPN1-EGFP (3)- or TAP-GFP (4)-expressing cells with or without infection. In noninfected cells, PABPN1-EGFP-containing nuclear speckles were distributed randomly, whereas in infected cells at 24 h p.i., they localized close to the nuclear membrane (Fig. 4A and G). TAP-EGFP, distributed homogeneously in nuclei of noninfected cells, localized in infected cells at the viral replication compartment (Fig. 4D). The FRAP of PABPN1-EGFP was slower in infected than noninfected cells (Fig. 4B and C), suggesting either slow diffusion or more-frequent binding to mRNA poly(A) tails. In Virtual Cell simulations, the theoretical diffusion constants of PABPN1-EGFP and mRNA were set at 22 and 0.04 $\mu m^2/s$, with partial binding of PABN1-EGFP to immobile speckle domains. The best fit yielded PABPN1-EGFP free diffusion, mRNA binding, and speckle binding times of 0.1, 2.5, and 50 s, respectively. The fit of PABPN1-EGFP recovery simulation in infected cells was good, with 10-times-higher mRNA binding on-rate and adjusted speckle binding parameters (Fig. 4C). In this case, the free diffusion time for PABPN1-EGFP, mRNA binding time, and speckle binding time were 0.01, 2.5, and 1,000 s, respectively. These models suggest that, during infection, PABPN1-EGFP diffuses freely for only a short time and binds to mRNA or speckle domains faster (10 times higher on-rate) and more strongly.

Interestingly, the rates of TAP-GFP fluorescence recovery were identical in noninfected and infected cells (Fig. 4E). The recovery fitted to the free diffusion model, yielding a diffusion coefficient of $2.2 \pm 0.3\ \mu m^2\ s^{-1}$. Mass scaling of the EGFP diffusion coefficient suggested that TAP-EGFP showed effective diffusion behavior (43), with 83% of TAP-EGFP bound and the rest freely diffusing (Fig. 4F).

Our previous studies demonstrated accumulation of CPV NS1 and viral DNA into the nuclear replication body and marginalization of host cell chromatin to the nuclear periphery (24, 25). Here we observed the time-dependent increase in NS1 mRNA production. At the same time, the amount of cellular mRNA was unaltered and that of cytoplasmic nascent RNA decreased. These findings imply that viral gene expression and virus-induced chromatin marginalization do affect cellular RNA dynamics.

In this study, photobleaching techniques were used to assess interactions between nuclear transcription-related proteins and viral components. FRAP studies exploring the dynamics of TBP, a protein essential for transcription initiation (2), demonstrated faster binding and release in infected than in noninfected cells. TBP interacts with TBP-associated factors to form the *TFIID* complex, which binds to chromosomal histone H3 (47). At late stages of infection, histone H3 is concentrated at the nuclear periphery, which could explain the weaker binding and the decreased binding time of TBP in the viral replication body area (E. A. Niskanen, O. Kalliolinna, T. O. Ihalainen, M. Vuokko, and M. Vihinen-Ranta, et al., unpublished data). The shorter free diffusion time, in turn, may be due to the relative increase in TBP binding sites in the replication body area. In parallel, infection did not affect PML recovery kinetics. These results suggested that, in contrast to some other viruses (1, 16, 17), PML bodies are not affected in CPV infection.

As in previous studies (6), TFIIB, also required in transcription initiation, showed shorter binding times than TBP in noninfected cells. The measured binding time reflects the time of preinitiation complex binding with TFIIB and polymerase II association with the promoter (15). In infected cells, TFIIB accumulated into to the replication body area and the binding time was similar to that in control cells, although the association rate was higher. The amount of TFIIB-EGFP was not affected by infection (our unpublished result), and the faster association indicates that transcription initiations are more frequent in infected cells. Based on these data, together with our previous studies, we propose a model for CPV infection progression in which the replication body grows and fills the nucleus. In parallel, the host cell chromatin is marginalized along with PML bodies and speckle domains. Inside the replication body, transcription is initiated more often than in noninfected cells, leading to a accumulation of the viral NS1 mRNA (Fig. 5).

In infected cells at 24 h p.i., PABPN1-EGFP localized to the splicing speckle domains (4, 5) and diffusively to the replication body area. FRAP experiments with virtual cell simulations in infected cells pointed to faster mRNA binding, however, with a longer residence time in the speckle domains.

TAP, an mRNA export protein interacting with nucleoporins and polyadenylated mRNA (12, 44), accumulated in the viral rep-

lication body area. The FRAP of TAP in noninfected cells was similar to that in infected cells. The diffusion coefficient of 2.2 ± 0.3 $\mu m^2/s$ of TAP (70 kDa) (33) was 6.5 times too small to correspond to free diffusion. However, the recovery data fitted well with the free diffusion model and collectively imply that the binding/unbinding reactions are extremely fast and that the recovery resembles that seen with slow diffusion. It previously has been reported that inside the nucleus, TAP diffused freely, with a diffusion coefficient of 1.2 ± 0.07 $\mu m^2/s$ (5). Together, these results suggest that binding of TAP to mRNA is transient.

ACKNOWLEDGMENTS

We thank Colin Parrish for the infectious CPV clone and antibodies, R. Everett for PML(IV)-EYFP, J. Langowski for H2B-ECFP, S. Huang for TBP-EGFP, M. Carmo-Fonseca for PABN1-EGFP and TAP-EGFP constructs, and Klaus Hedman for comments on the manuscript. The first-class experimental support of Milla Häkkinen, Jenni Reimari, and Irene Helkala is gratefully acknowledged.

The work was supported by grants from the Academy of Finland (Contracts 129774 and 138388), National Graduate School in Nano-Science, and National Graduate School in Informational and Structural Biology.

REFERENCES

1. **Ahn JH, Brignole EJ, Hayward GS.** 1998. Disruption of PML subnuclear domains by the acidic IE1 protein of human cytomegalovirus is mediated through interaction with PML and may modulate a RING finger-dependent cryptic transactivator function of PML. Mol. Cell. Biol. **18**: 4899–4913.
2. **Albright SR, Tjian R.** 2000. TAFs revisited: more data reveal new twists and confirm old ideas. Gene **242**:1–13.
3. **Bachi A, et al.** 2000. The C-terminal domain of TAP interacts with the nuclear pore complex and promotes export of specific CTE-bearing RNA substrates. RNA **6**:136–158.
4. **Calado A, Carmo-Fonseca M.** 2000. Localization of poly(A)-binding protein 2 (PABP2) in nuclear speckles is independent of import into the nucleus and requires binding to poly(A) RNA. J. Cell Sci. **113**:2309–2318.
5. **Calapez A, et al.** 2002. The intranuclear mobility of messenger RNA binding proteins is ATP dependent and temperature sensitive. J. Cell Biol. **159**:795–805.
6. **Chen D, Hinkley CS, Henry RW, Huang S.** 2002. TBP dynamics in living human cells: constitutive association of TBP with mitotic chromosomes. Mol. Biol. Cell **13**:276–284.
7. **Chen D, Huang S.** 2001. Nucleolar components involved in ribosome biogenesis cycle between the nucleolus and nucleoplasm in interphase cells. J. Cell Biol. **153**:169–176.
8. **Chen IH, Sciabica KS, Sandri-Goldin RM.** 2002. ICP27 interacts with the RNA export factor Aly/REF to direct herpes simplex virus type 1 intronless mRNAs to the TAP export pathway. J. Virol. **76**:12877–12889.
9. **Chen Z, Krug RM.** 2000. Selective nuclear export of viral mRNAs in influenza-virus-infected cells. Trends Microbiol. **8**:376–383.
10. **Chen Z, Li Y, Krug RM.** 1999. Influenza A virus NS1 protein targets poly(A)-binding protein II of the cellular 3′-end processing machinery. EMBO J. **18**:2273–2283.
11. **Christensen J, Cotmore SF, Tattersall P.** 1995. Minute virus of mice transcriptional activator protein NS1 binds directly to the transactivation region of the viral P38 promoter in a strictly ATP-dependent manner. J. Virol. **69**:5422–5430.
12. **Conti E, Izaurralde E.** 2001. Nucleocytoplasmic transport enters the atomic age. Curr. Opin. Cell Biol. **13**:310–319.
13. **Cotmore SF, Christensen J, Nuesch JP, Tattersall P.** 1995. The NS1 polypeptide of the murine parvovirus minute virus of mice binds to DNA sequences containing the motif [ACCA]2–3. J. Virol. **69**:1652–1660.
14. **Czepluch C, et al.** 2000. H-1 parvovirus-associated replication bodies: a distinct virus-induced nuclear structure. J. Virol. **74**:4807–4815.
15. **Darzacq X, et al.** 2007. In vivo dynamics of RNA polymerase II transcription. Nat. Struct. Mol. Biol. **14**:796–806.
16. **Everett RD, et al.** 2006. PML contributes to a cellular mechanism of repression of herpes simplex virus type 1 infection that is inactivated by ICP0. J. Virol. **80**:7995–8005.
17. **Everett RD.** 2001. DNA viruses and viral proteins that interact with PML nuclear bodies. Oncogene **20**:7266–7273.
18. **Fontaine-Rodriguez EC, Knipe DM.** 2008. Herpes simplex virus ICP27 increases translation of a subset of viral late mRNAs. J. Virol. **82**:3538–3545.
19. **Fontaine-Rodriguez EC, Taylor TJ, Olesky M, Knipe DM.** 2004. Proteomics of herpes simplex virus infected cell protein 27: association with translation initiation factors. Virology **330**:487–492.
20. **Fraefel C, et al.** 2004. Spatial and temporal organization of adeno-associated virus DNA replication in live cells. J. Virol. **78**:389–398.
21. **Geisberg JV, Lee WS, Berk AJ, Ricciardi RP.** 1994. The zinc finger region of the adenovirus E1A transactivating domain complexes with the TATA box binding protein. Proc. Natl. Acad. Sci. U. S. A. **91**:2488–2492.
22. **Green M, Panesar NK, Loewenstein PM.** 2008. The transcription-repression domain of the adenovirus E1A oncoprotein targets p300 at the promoter. Oncogene **27**:4446–4455.
23. **Hagemeier C, Walker S, Caswell R, Kouzarides T, Sinclair J.** 1992. The human cytomegalovirus 80-kilodalton but not the 72-kilodalton immediate-early protein transactivates heterologous promoters in a TATA box-dependent mechanism and interacts directly with TFIID. J. Virol. **66**: 4452–4456.
24. **Hall DB, Struhl K.** 2002. The VP16 activation domain interacts with multiple transcriptional components as determined by protein-protein cross-linking in vivo. J. Biol. Chem. **277**:46043–46050.
25. **Ihalainen TO, et al.** 2009. Parvovirus induced alterations in nuclear architecture and dynamics. PLoS One **4**:e5948. doi:10.1371/journal.pone.0005948.
26. **Ihalainen TO, et al.** 2007. Dynamics and interactions of parvoviral NS1 protein in the nucleus. Cell. Microbiol. **9**:1946–1959.
27. **Jenal M, et al.** 2012. The poly(A)-binding protein nuclear 1 suppresses alternative cleavage and polyadenylation sites. Cell **149**:538–553.
28. **Johnson LA, Sandri-Goldin RM.** 2009. Efficient nuclear export of herpes simplex virus 1 transcripts requires both RNA binding by ICP27 and ICP27 interaction with TAP/NXF1. J. Virol. **83**:1184–1192.
29. **Jul-Larsen A, et al.** 2004. PML-nuclear bodies accumulate DNA in response to polyomavirus BK and simian virus 40 replication. Exp. Cell Res. **298**:58–73.
30. **Kashanchi F, et al.** 1994. Direct interaction of human TFIID with the HIV-1 transactivator tat. Nature **367**:295–299.
31. **Kim JM, Hong Y, Jeang KT, Kim S.** 2000. Transactivation activity of the human cytomegalovirus IE2 protein occurs at steps subsequent to TATA box-binding protein recruitment. J. Gen. Virol. **81**:37–46.
32. **Lee WS, Kao CC, Bryant GO, Liu X, Berk AJ.** 1991. Adenovirus E1A activation domain binds the basic repeat in the TATA box transcription factor. Cell **67**:365–376.
33. **Liker E, Fernandez E, Izaurralde E, Conti E.** 2000. The structure of the mRNA export factor TAP reveals a cis arrangement of a non-canonical RNP domain and an LRR domain. EMBO J. **19**:5587–5598.
34. **Liljelund P, Ingles CJ, Greenblatt J.** 1993. Altered promoter binding of the TATA box-binding factor induced by the transcriptional activation domain of VP16 and suppressed by TFIIA. Mol. Gen. Genet. **241**:694–699.
35. **Maul GG, Ishov AM, Everett RD.** 1996. Nuclear domain 10 as preexisting potential replication start sites of herpes simplex virus type-1. Virology **217**:67–75.
36. **Niskanen EA, Ihalainen TO, Kalliolinna O, Häkkinen MM, Vihinen-Ranta M.** 2010. Effect of ATP binding and hydrolysis on dynamics of canine parvovirus NS1. J. Virol. **84**:5391–5403.
37. **Nüesch JP, Cotmore SF, Tattersall P.** 1995. Sequence motifs in the replicator protein of parvovirus MVM essential for nicking and covalent attachment to the viral origin: identification of the linking tyrosine. Virology **209**:122–135.
38. **Qadri I, Maguire HF, Siddiqui A.** 1995. Hepatitis B virus transactivator protein X interacts with the TATA-binding protein. Proc. Natl. Acad. Sci. U. S. A. **92**:1003–1007.
39. **Raha T, Cheng SW, Green MR.** 2005. HIV-1 tat stimulates transcription complex assembly through recruitment of TBP in the absence of TAFs. PLoS Biol. **3**:e44. doi:10.1371/journal.pbio.0030044.
40. **Sandri-Goldin RM.** 2004. Viral regulation of mRNA export. J. Virol. **78**:4389–4396.

41. **Soliman TM, Silverstein SJ.** 2000. Herpesvirus mRNAs are sorted for export via Crm1-dependent and -independent pathways. J. Virol. **74**: 2814–2825.
42. **Sourvinos G, Everett RD.** 2002. Visualization of parental HSV-1 genomes and replication compartments in association with ND10 in live infected cells. EMBO J. **21**:4989–4997.
43. **Sprague BL, Pego RL, Stavreva DA, McNally JG.** 2004. Analysis of binding reactions by fluorescence recovery after photobleaching. Biophys. J. **86**:3473–3495.
44. **Strawn LA, Shen T, Wente SR.** 2001. The GLFG regions of Nup116p and Nup100p serve as binding sites for both Kap95p and Mex67p at the nuclear pore complex. J. Biol. Chem. **276**:6445–6452.
45. **Tang Q, Bell P, Tegtmeyer P, Maul GG.** 2000. Replication but not transcription of simian virus 40 DNA is dependent on nuclear domain 10. J. Virol. **74**:9694–9700.
46. **Tsao J, et al.** 1991. The three-dimensional structure of canine parvovirus and its functional implications. Science **251**:1456–1464.
47. **Vermeulen M, et al.** 2007. Selective anchoring of TFIID to nucleosomes by trimethylation of histone H3 lysine 4. Cell **131**:58–69.
48. **Veschambre P, Simard P, Jalinot P.** 1995. Evidence for functional interaction between the HIV-1 tat transactivator and the TATA box binding protein in vivo. J. Mol. Biol. **250**:169–180.
49. **Wang YC, Huang CF, Tung SF, Lin YS.** 2000. Competition with TATA box-binding protein for binding to the TATA box implicated in human cytomegalovirus IE2-mediated transcriptional repression of cellular promoters. DNA Cell Biol. **19**:613–619.
50. **Young PJ, Jensen KT, Burger LR, Pintel DJ, Lorson CL.** 2002. Minute virus of mice NS1 interacts with the SMN protein, and they colocalize in novel nuclear bodies induced by parvovirus infection. J. Virol. **76**:3892–3904.
51. **Young PJ, et al.** 2005. Minute virus of mice small non-structural protein NS2 localizes within, but is not required for the formation of, Smn-associated autonomous parvovirus-associated replication bodies. J. Gen. Virol. **86**:1009–1014.
52. **Zabierowski SE, Deluca NA.** 2008. Stabilized binding of TBP to the TATA box of herpes simplex virus type 1 early (tk) and late (gC) promoters by TFIIA and ICP4. J. Virol. **82**:3546–3554.